Drugs modifications: Graphene oxide-chitosan loading enhanced anti-amoebic effects of pentamidine and doxycycline

Tooba Jabri[1], Meshal Daalah[2], Bader S. Alawfi[3], Jasra Gul[1], Usman Ahmed[4], Muhammad Raza Shah[1], Naveed Ahmed Khan[5,6*], Ruqaiyyah Siddiqui[6,7*], Tan Yee Ying[4], Yeo Jia Tong[4], Ayaz Anwar[4]*

[1]H. E. J. Research Institute of Chemistry, International Center for Chemical and Biological Sciences, University of Karachi, Karachi 75270, Pakistan; [2]Department of Medical Laboratory Sciences, Faculty of Allied Health Sciences, Health Sciences Center, Kuwait University, Jabriya, Kuwait; [3]Department of Medical Laboratories Technology, College of Applied Medical Sciences, Taibah University, Madinah 42353, Saudi Arabia; [4]Department of Biological Sciences, School of Medical and Life Sciences, Sunway University, Subang Jaya 47500, Selangor, Malaysia; [5]School of Science, College of Science and Engineering, University of Derby, Derby, DE22 1GB, UK; [6]Microbiota Research Center, Istinye University, Istanbul, 34010, Turkey; [7]Institute of Biological Chemistry, Biophysics and Bioengineering, Heriot-Watt University Edinburgh, EH14 4AS UK.

Short title: Drug modification and anti-*A. castellanii*

Corresponding address: A. Anwar, Department of Biological Sciences, School of Medical and Life Sciences, Sunway University, Subang Jaya 47500, Selangor, Malaysia; **N. A. Khan**: School of Science, College of Science and Engineering, University of Derby, Derby, DE22 1GB, UK.

Abstract

Acanthamoeba castellanii is the causative pathogen of a severe eye infection, known as *Acanthamoeba* keratitis and a life-threatening brain infection, named granulomatous amoebic encephalitis. Current treatments are problematic, costly and exhibit limited efficacy against the *Acanthamoeba* parasite, especially the cyst stage. In parallel to drug discovery and drug repurposing efforts, drug modification is an important approach to tackle infections, especially against neglected parasites such as the free-living amoeba: *Acanthamoeba*. In this study, we determined whether modifying pentamidine and doxycycline through chitosan-functionalized graphene oxide loading, enhances their anti-amoebic effects. Various concentrations of doxycycline, pentamidine, graphene oxide, chitosan-functionalized graphene oxide and chitosan-functionalized graphene oxide loaded with doxycycline and pentamidine were investigated for amoebicidal effects against pathogenic *A. castellanii* belonging to the T4 genotype. Lactate dehydrogenase assays were performed to determine toxic effects of these various drugs and nanoconjugates against human cells. The findings revealed that chitosan-functionalized graphene oxide loaded with doxycycline demonstrated potent amoebicidal effects. Nanomaterials also significantly ($p < 0.05$) inhibited excystation and encystation of *A. castellanii* without exhibiting toxic effects against human cells in a concentration-dependent manner, as compared with the other formulations. These results indicate that drug modifications, coupled with nanotechnology maybe a viable avenue in the rationale development of effective therapies against *Acanthamoeba* infections.

Keywords: Drug modification; Graphene oxide; Chitosan; Doxycycline; Pentamidine; *Acanthamoeba*.

Introduction

The unicellular pathogenic *Acanthamoeba* spp. are associated with keratitis and encephalitis (Marciano-Cabral and Cabral 2003; Clarke and Niederkorn, 2006; Khan 2006; Visvesvara et al. 2007; Panjwani, 2010; Rayamajhee et al., 2024). Given the rarity of the infections caused by *Acanthamoeba* and the limited number of cases reported, the development of therapeutic strategies has largely been neglected by the pharmaceutical industry. Thus the onus is on the academic community to develop therapeutic interventions or at the very least identify potential drug leads (Debnath, 2021). Novel drug discovery efforts are costly, requiring funds in millions ($). However, most funding agencies that support academic researchers, fund projects in the range of thousands ($), and that too in specific priority areas of major diseases. Having said this, it is promising that many researchers are investigating amoebal pathogens, with an eye to identify potential anti-amoebic molecules of therapeutic value and these efforts are strongly encouraged. To overcome funding challenges, researchers have turned to drug repurposing and drug modifications of existing drugs to expedite discovery of lead compounds (Elsheikha et al., 2021; Debnath, 2021). For the latter, biguanide, diamidine, and azole are currently prescribed in combination against *Acanthamoeba* infections (Clarke and Niederkorn, 2006; Visvesvara et al., 2007; Panjwani, 2010). For instance, chlorhexidine gluconate (CHX) as well as pentamidine (Pent) are one of the widely used biguanides and diamidines respectively. Chlorhexidine has been used extensively; however, it is also reported that failure on the bioavailability of the drug tends to occur in the corneal stroma (Sangkanu et al., 2021). On the other hand, Pent is a well-known drug against *Acanthamoeba* spp. Pentamidine disrupts the biosynthesis of nucleic acids and proteins, to exert its' effects (Elsheikha et al., 2020; Siddiqui et al. 2016). Nevertheless, the use of Pent has been found to carry potential neurotoxicity due to

poor specificity (Sanderson et al., 2021). Additionally, the blood-brain barrier which is highly selective can impede drug delivery into the central nervous system and act as another obstacle in the therapy of amoebic infections (Ong et al., 2017). Moreover, there are growing risks of developing multi-drug resistance in *Acanthamoeba* which need to be addressed in advance (Turner et al., 2004; Henriquez et al., 2021). Hence, we investigate if a "drug modification approach" can be utilized to increased efficacy of known drugs such as Pent.

Carbon-based nano-structured materials, such as carbon nanotubes (CNTs), Buckminster fullerenes (C60), carbon dots (CDs), and graphene and its derivatives, are known for their distinctive mechanical and biological properties (Chiu et al., 2018). Among these, graphene oxide (GO) is particularly notable for its monolayer, two-dimensional honeycomb crystal structure, which provides a vast specific surface area and an array of polar functional groups. These features make GO and its derivatives promising as drug carriers, facilitating drug transport through surface adsorption, hydrogen bonding, electrostatic interactions (Kumar et al., 2021), and exhibits biological properties such as anti-cancerous activities, textile dye remediation etc. (Biswas et al., 2023; Keerthana et al., 2022). GO's mechanical properties enable functionalization through both covalent and non-covalent interactions, while its capacity to cross-link with diverse polymers amplifies the biological potential of GO-based polymeric nanocomposites. Consequently, the development of aqueous-dispersible, biocompatible, and non-toxic graphene oxide-based polysaccharides holds paramount importance for drug delivery applications (Feng and Wang, 2022). Natural polymers such as chitosan (CHI), characterized by its linear cationic biopolymer structure comprising glucosamine and N-acetylglucosamine, emerge as particularly promising candidates in biomedical contexts due to their inherent biocompatibility and biodegradability. Extensive biological applications, including antibacterial, anti-inflammatory, antioxidant, and

immunomodulatory properties, underscore the significance of chitosan and its derivatives in biomedical research (Wang et al., 2020).

The biodegradable nature, low immunogenicity, and biocompatibility of these materials make them suitable for drug delivery, cell adhesion, tissue engineering, and gene delivery (Deb and Vimala, 2018; Motiei and Kashanian, 2017). The combination of chitosan with graphene oxide has resulted in materials with unique functionalities, especially as nanocarriers for drug delivery. For example, Su et al. (2021) developed silver nanoparticle-infused GO nanocomposites with antimicrobial properties capable of multi-drug release. Keasavan et al. (2021) created a formulation of CHI and D-mannose functionalized GO to deliver Ulvan for targeted anticancer therapy. Doxycycline (Doxy), a broad-spectrum tetracycline antibiotic, is used for treating various infectious diseases and has demonstrated anticancer properties by inhibiting matrix metalloproteinases (Singh and Nenavathu, 2020).

Recent research has explored Doxy's use in treating COVID-19 and it has shown efficacy against Dengue and Chikungunya viruses (Malek et al., 2020; Narendrakumar et al., 2021). Additionally, Doxy has been effective against *A. castellanii* (Jha et al., 2015). Pentamidine isethionate has been used to treat several parasitic infections such as leishmaniasis, pneumocystis, trypanosomiasis, and babesiosis (Peretti et al., 2018; Kannan et al., 2021). Although its primary mechanism of action is not fully understood, Pentamidine binds to adenine-thymine rich DNA regions, facilitated by its terminal amidine groups and aromatic rings, which enable intercalation and stabilization within the DNA double helix (Peretti et al., 2018). Pentamidine and its derivatives have shown potent amoebicidal activity against species like *A. castellanii*, *A. polyphaga*, and *A. hatchetti* (Alizadeh et al., 1997). This study aims to investigate

whether modifying Pent and Doxy with chitosan-functionalized graphene oxide enhances their anti-amoebic effects.

Materials and Methods

Graphite was sourced from AVONCHEM, while chitosan, pentamidine, doxycycline hyclate, phosphoric acid, ethanol, and diethyl ether were sourced from Sigma Aldrich. 1-ethyl-3-[3-(dimethylamino)propyl] carbodiimide hydrochloride was obtained from Ambeed, sulfuric acid and hydrochloric acid were procured from BDH labs. Potassium permanganate and hydrogen peroxide were purchased from Scharlau Chemicals.

Graphene oxide synthesis

Graphene oxide was synthesized using Hummer's method as previously described (Shahriary & Athawale, 2014). Briefly, 9:1 mixture of H_2SO_4 and H_3PO_4 was added to graphite (3g, 1 equivalent), followed by stirring for 10min. Next, $KMnO_4$ (18.0g, 6 equivalent) was added. The mixture was agitated for 12h at 50°C, and then poured onto ice. Subsequently, 30% H_2O_2 (3mL) was added in a dropwise manner and centrifuged at 4,000 x rpm for 1h. After this, the supernatant was discarded and the solid residue was sequentially washed with H_2O (300mL), 30% HCl (300mL×2), and ethanol (×2). During each washing, samples were centrifuged at 4,000 x rpm for 1h and the resulting product was coagulated with ether, filtered, and vacuum dried at ambient temperature. Finally, graphene oxide was sonicated to produce nano-graphene oxide.

Graphene oxide functionalized with chitosan

Graphene oxide was functionalized with chitosan through an amidation reaction. Briefly, GO (1mg/mL, 50mL) was sonicated for homogeneous nano-suspension for 1h. Next, EDC (150mg) and NHS (75mg) were added and stirred overnight to activate the carboxyl groups on GO. After this, CHI (1% wt) was added, and the mixture was stirred overnight at room temperature and then centrifuged and washed with water to eliminate any unreacted CHI. The resulting product, GO-CHI, was lyophilized for experimentation.

Drug loaded GO-CHI nanocarrier

Doxycycline (Doxy) and pentamidine (Pent) were loaded onto GO-CHI nanocarriers. Initially, by dissolving Doxy in water and Pent in methanol, each at a concentration of 0.5mg/mL with a total volume of 10 mL for each drug. These drugs were then separately added to two distinct GO-CHI solutions (1 mg/ mL), and stirred continuously at 500 x rpm for 24h. Next, the drug-loaded solutions underwent centrifugation to separate the GO-CHI nanocarrier from the free drug. The amount of unbound drug in the supernatant was measured to calculate the drug loading efficiency. The efficiency of drug loading was assessed using the following formula: Drug-loading efficiency = (total drug–unbound drug) / total drug ×100.

Analysis using Fourier Transform Infrared (FTIR) Spectroscopy

To investigate interactions, FTIR analysis was carried out using Nicolet 6700 FTIR spectrometer (Thermo Nicolet), equipped with a deuterated triglycine sulphate detector and operated via OMNIC operating system software, spectra were acquired as described in our earlier studies (Anwar et al., 2019a; 2019b). Samples were directly placed in contact with

attenuated total reflectance (ATR) on a ZnSe plate at room temperature. Spectra were recorded across the range of 4500-650 cm^{-1}, comprising 16 scans at a resolution of 4 cm^{-1}.

Atomic force microscopy (AFM) and scanning electron microscopy (SEM)

Analysis of GO, GO-CHI, GO-CHI-Doxy and GO-CHI-Pent was carried out by atomic force microscopy **(**Agilent, USA), and scanning electron microscope ((JEOL-JSM-6380A) as previously described (Anwar et al., 2019a; 2019b). For AFM, samples were diluted and placed on mica slide, air dried, and mounted on microscope. Scanning of images was accomplished in non-contact mode. SEM analysis was also conducted to investigate the ultramicroscopic features of these nanocomposites. Samples were mounted on a metallic stub and sputter coated with a thin layer of gold to enhance conductivity. Images were captured at a 5000 x, with a scale bar of 10 µm.

Thermal stability, X-Ray diffraction, and Zeta potential analysis

Thermal stability of samples was assessed through thermogravimetric analysis using a TA instrument, SDT650 as described earlier (Anwar et al., 2019a; 2019b). Thermal screening was carried out across a heating range of 25°C-800°C, with heating rate of 15°C per min under nitrogen atmosphere. Additionally, nano formulations were explored for Zeta potential using a Zetasizer instrument (ZS-90, UK) as described before (Anwar et al., 2019a; 2019b). Samples were incorporated into deionized water, and then data were obtained in triplicates. Powdered X-ray diffraction (PXRD) analysis was performed for GO, CHI, and GO-CHI nanocomposites on a Xpert pro, PANaltyical diffractometer with Cu Kα (λ =1.5418 Å) as previously (Anwar et al., 2019a; 2019b).

178 ***Acanthamoeba castellanii* culture**

179 The growth medium (PYG) was formulated by combining 0.75% proteose peptone,
180 0.75% yeast extract, and 1.5% glucose. *Acanthamoeba castellanii* trophozoites were obtained
181 from a keratitis patient (ATCC 50492) were routinely cultured in tissue culture flasks at 30°C
182 and monitored until confluency was reached as previously described (Anwar et al., 2019a).

183 **Amoebicidal Assay**

184 The stock solution of GO-CHI-Doxy, GO-CHI-Pent, GO, and GO-CHI were prepared at
185 10mg/mL in ddH_2O. *Acanthamoeba castellanii* were collected by centrifugation at 3,000 x rpm
186 for 10min. Next, amoebae were suspended in RPMI-1640 and exposed to various concentrations
187 of GO-CHI-Doxy (25, 50, and 100µg/mL), GO-CHI-Pent (25, 50, and 100µg/mL), GO (25, 50,
188 and 100µg/mL), and GO-CHI (25, 50, and 100µg/mL). Chlorhexidine (100µg/mL) alone was
189 used as a positive control, while ddH_2O was used as a solvent control. Amoebae were incubated
190 at 30°C for 24h. Following incubation, Trypan blue exclusion assay was employed to enumerate
191 unstained viable cells using a hemocytometer (Ahmed et al., 2023a). The number of amoebae
192 incubated alone was considered as 100% and relative percent viability was determined
193 accordingly.

194 **Cysts formation and excystation assay**

195 The trophozoites were transformed into mature cysts by transferring healthy trophozoites
196 to non-nutrient agar (NNA) plates. Briefly, trophozoites were tapped and centrifuged at 3,000 x
197 rpm for 10min. The pellet was resuspended in 1mL of PBS and inoculated on NNA plates. The
198 plates were properly labelled and incubated at 30°C for 15 days. The cells were observed under
199 an inverted microscope, until they transformed into mature cysts.

Excystation assays were performed as described earlier (Ahmed et al., 2023b). The cysts were counted, and the concentration was adjusted to 1 x 10^5 cells per well using a haemocytometer. The cysts were treated with various concentrations of GO-CHI-Doxy (25, 50, and 100µg/mL), GO-CHI-Pent (25, 50, and 100µg/mL), GO (25, 50, and 100µg/mL), and GO-CHI (25, 50, and 100µg/mL). Chlorhexidine (100µg/mL) alone was used as a positive control, while ddH_2O was used as a solvent control. The cells were incubated for 72 hours at 30°C in excystation media. After the assigned duration of incubation, the newly emerged trophozoites were counted under an inverted microscope by using Trypan blue exclusion assay.

Encystation assay

The tested compounds were also assessed for their possible activity to inhibit the transformation of trophozoites into cysts/encystation. The assay was performed as described earlier (Ahmed et al., 2023b), The trophozoites were enumerated and treated in encystment (glucose, PBS + Pen strip, $MgCl_2$) medium with various concentrations of GO-CHI-Doxy (25, 50, and 100µg/mL), GO-CHI-Pent (25, 50, and 100µg/mL), GO (25, 50, and 100µg/mL), and GO-CHI (25, 50, and 100µg/mL). Chlorhexidine (100µg/mL) alone was used as a positive control, while ddH_2O was used as a solvent control. The trophozoites were treated for 72 hours. Next, the cells were treated with 0.25% SDS for 2 minutes to dissolve trophozoites and immature cysts. Only mature cysts were counted under an inverted microscope.

Human cell culture and lactate dehydrogenase assay

Human keratinocyte skin cells (HaCaT) were grown in tissue culture flasks containing 10 mL of growth media (RPMI-1640 containing 10% fetal bovine serum, glutamine, 100 U/mL penicillin, 100 µg/mL streptomycin, and 1% non-essential amino acid as previously described (Anwar et al., 2019a; 2019b). Once a complete monolayer was formed, human cells were washed

with PBS to eliminate any dead cells. Next, trypsin (ca. 2 mL) was added to each flask and incubated for 10 min at 37°C. Next, cells were centrifuged at 1,500 x rpm for 5 min, and the pellet was suspended in RPMI (Anwar et al., 2019b). For assays, HaCaT cells were grown in 96-well plates and exposed to drugs. Next, cells plus drugs were subjected to 24 h of incubation at 37°C with 5% CO_2. After this incubation, supernatants were harvested, and the amount of released lactate dehydrogenase (LDH) was determined using a cytotoxicity detection kit. Briefly, equal volumes of sample and LDH assay reagent (50 µL each) were mixed in 96-well plates. The plates were then incubated at room temperature in the dark for 20 min and then read using a plate reader with a reference wavelength of 490 nM. The results were calculated as follows: % cell cytotoxicity = (sample value – negative control value) / (positive control value, i.e., 1% Triton X-100 treated – negative control value) × 100. Untreated HaCaT cells were used as negative control, while 1% Triton X-100 were used as positive control as previously described (Jeyamogan et al., 2018).

Statistical analysis

Two-sample T-test and a two-tailed distribution were employed to ascertain significant differences between the means of two independent data groups, utilizing Microsoft Excel. Data analysis was conducted with a critical value set at < 0.05. Additionally, on graphical representations, the y-axis errors denoted the standard error of each data point in the graph. Notably, significance levels were indicated as follows: *, indicating $p < 0.05$.

Results

Graphene oxide was successfully synthesized using an enhanced version of Hummer's method, followed by exfoliation through sonication to produce graphene oxide nanoparticles

(Marcano et al., 2010). These nanoparticles were then subjected to covalent interaction with chitosan (CHI) through amide linkage, resulting in the formation of graphene oxide chitosan (GO-CHI), as depicted in Scheme 1a. Subsequently, the biocompatible GO-CHI was employed as a nanocarrier for loading the tetracycline antibiotic doxycycline (GO-CHI-Doxy) and the antimicrobial agent pentamidine (Pent), as illustrated in Scheme 1b.

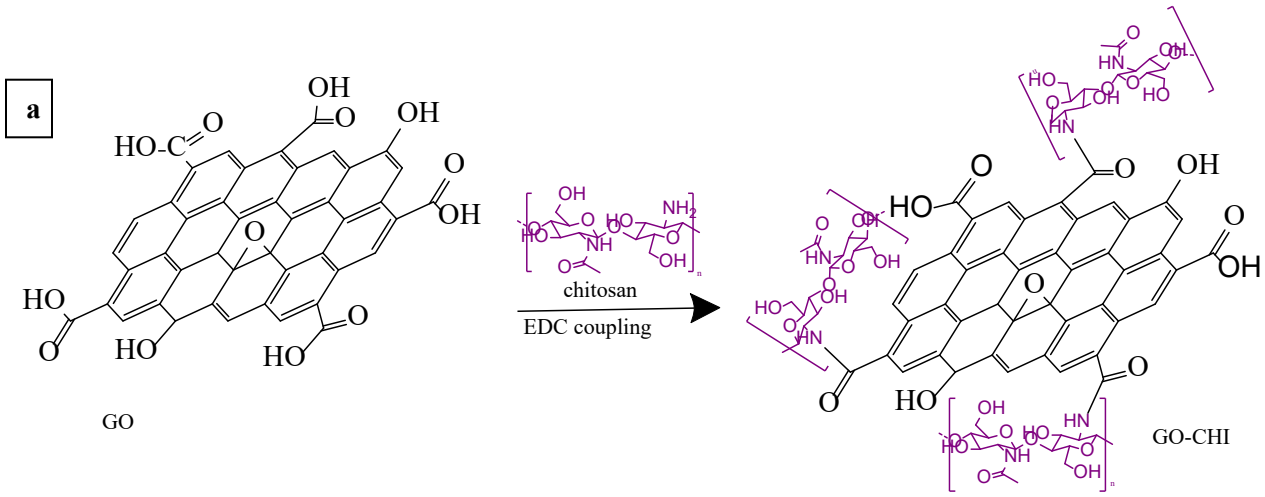

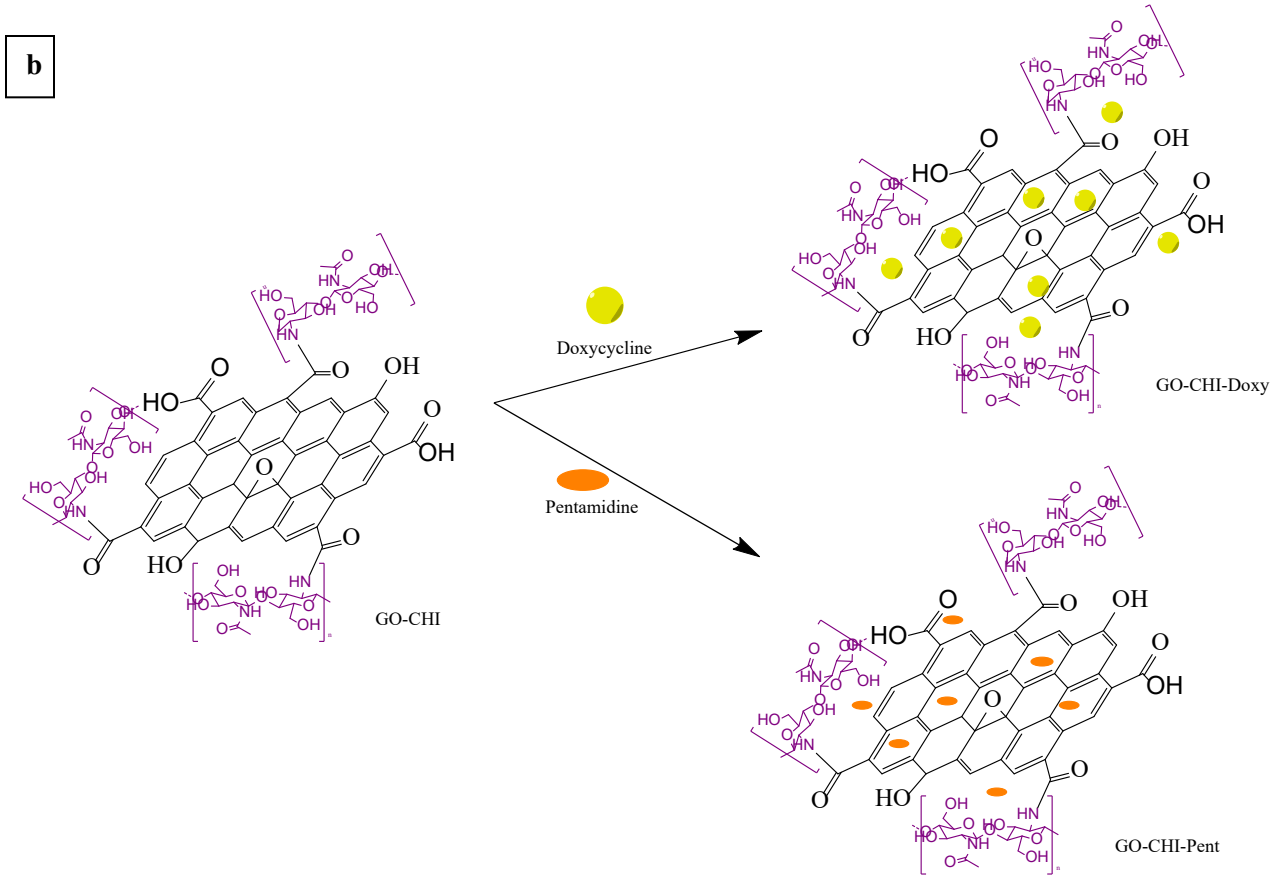

Scheme 1: (a) Synthesis of GO-CHI (b) Drugs loaded GO-CHI (GO-CHI-Doxy and GO-CHI-Pent).

FTIR

Figure 1 provides a comprehensive view of the FTIR spectra, elucidating interactions within the nanocomposites GO, GO-CHI, GO-CHI-Doxy, and GO-CHI-Pent. In Figure 1a, the GO spectrum reveals characteristic vibrations, including –OH stretching around 3400-3300 cm^{-1}, and –C=O stretching at 1730 cm^{-1}. CHI spectrum exhibits peaks at 3360 cm^{-1} attributed to N-H stretching. Notably, GO-CHI shows peaks at 1650 cm^{-1} and 1570 cm^{-1}, indicating amide coupling. In Figure 1b, doxycycline spectrum displays peaks corresponding to functional groups such as –NH and –OH. The FTIR spectra of GO-CHI-Doxy reveal shifts indicating interaction,

particularly in the amide and –C=O stretching regions. Figure 1c illustrates pentamidine's interaction with GO-CHI, characterized by distinct peaks attributed to its functional groups. GO-CHI-Pent shows broad peaks in the 3500-3200 cm^{-1} range, indicating interaction with Pent (Rana et al., 2011; Yadav et al., 2017; Safdar et al., 2022; Peretti et al., 2018).

Thermogravimetric analysis

Thermogravimetric analysis (TGA) was employed to investigate the thermal stability and behavior of pristine GO, pure chitosan, and GO modified by chitosan (GO-CHI), as shown in Fig 2. Thermogram indicates an initial weight loss between approximately 30°C and 100°C, representing about 15%, 9%, and 11% for GO, CHI, and GO-CHI, respectively, due to water evaporation. Following this, GO exhibits decreased thermal stability around 200°C, with a 70% weight loss attributed to the decomposition of oxygen species and carbon dioxide evolution. CHI's thermal decomposition occurs approximately between 250°C and 400°C after moisture loss, due to glycosidic unit degradation and depolymerization. However, the GO-CHI thermogram depicts weight loss of approximately 50% from 156°C to 350°C in two stages (Kumar and Koh, 2014). The thermal stability of GO-CHI is increased compared to pure GO, attributed to bond formation between chitosan and GO, resulting in a reduction in labile oxygen-containing functional groups.

Morphological Analysis

The morphology of GO, GO-CHI, GO-CHI-Doxy, and GO-CHI-Pent was scrutinized using AFM and SEM techniques as shown in Fig 3. SEM micrographs of graphene oxide nanoparticles unveil a rugged, irregularly wrinkled structure attributed to the presence of functional moieties like epoxy, hydroxyl, and acidic groups on the GO surface (Deng and Berry, 2016; Cheng et al.,

2019). AFM images corroborate these observations, revealing uneven, notched shapes, irregular surfaces, and roughness (Fig 3a) (Cheng et al., 2019). Additionally, chitosan-grafted graphene oxide nanoparticles exhibit a distinct morphology, featuring a smoother structure compared to GO, with chitosan clumps adhering to the graphene oxide's rough surface, as evidenced in SEM and AFM images (Fig 3b). Conversely, GO-CHI-Doxy and GO-CHI-Pent showcase spherical particles on the GO's rough surface, indicative of successful drug loading onto the GO-CHI nanocarrier, as illustrated in Fig 3(c-d).

X-Ray diffraction

An X-Ray diffractogram of the synthesized GO nanocomposite and chitosan-grafted graphene oxide (GO-CHI) nanocarrier is depicted in Fig 4. A sharp peak characteristic of GO at $2\theta = 9.45°$, corresponding to (001) crystal plane, which equates to an interlayer d-spacing of approximately 9.6 Å. This indicates the presence of oxygen-rich species at the basal plane of GO. Conversely, pure chitosan displays two distinct peaks around 9.23° and 20.3°, corresponding to d-spacing values of 9.5 Å and 4.37 Å, respectively. Upon functionalization of graphene oxide with chitosan (GO-CHI) nanocarrier, two peaks emerge at approximately 9.5° and 19.05°, with corresponding interlayer d-spacing values of 9.39 Å and 4.66 Å. This indicates the successful attachment of chitosan to the GO surface. The prominent peak at 9.5° in GO-CHI suggests the overlap of GO and CHI as described in previous studies (Han et al., 2011; El Rouby et al., 2018; Gong et al., 2019).

Zeta Potential

Zeta potential, a crucial parameter for assessing nanoparticle surface charge, varies based on the functional groups present on the nanoparticle surface (Veerapandian and Neethirajan,

2015). GO exhibited a surface charge of -27.0 mV due to the presence of carbonyl, hydroxyl, and epoxy functional groups. Following functionalization and subsequent electrostatic conjugation with drugs, the zeta potential shifted to relatively less negative magnitudes, approximately -19.4 mV for GO-CHI, -20.5 mV for GO-CHI-Doxy, and -21.2 mV for GO-CHI-Pent. This shift suggests the loss of carboxyl groups during surface modification via covalent linkage and electrostatic interactions.

Drug Encapsulation Studies

Doxycycline (Doxy) and Pentamidine (Pent) were loaded onto the surface of the GO-CHI nanocarrier. The entrapment efficiency of Doxy and Pent on GO-CHI was evaluated by isolating free drug through centrifugation, followed by quantification using a UV-vis spectrophotometer. The calculated entrapment efficiencies were found to be 80% for Doxy and 75% for Pent. Specifically, Doxy was loaded into GO-CHI nanocarrier at a concentration of 0.40 mg/mL, while Pent was loaded at a concentration of 0.375 mg / mL. These findings indicate that 80% Doxy and 75% Pent were effectively encapsulated by the GO-CHI nanocarriers, demonstrating substantial drug loading and retention within the nanocarrier system.

Nanoconjugates of doxycycline and pentamidine exhibited significant anti-amoebic effects

Figure 5 demonstrates a clear decrease in viable cell counts with increasing concentrations of test samples. Specifically, the cell numbers followed the trend of GO-CHI-Doxy < GO-CHI < GO at each concentration. These observations revealed statistical significance ($p<0.05$) (Fig. 5). The IC_{50} of GO-CHI-Doxy against *A. castellanii* ranged between 25µg/mL and 50µg/mL, indicating lower efficacy compared to Doxy alone. At a concentration of 100µg/mL, the parasite number treated with GO-CHI-Doxy reduced further from that of pure GO. Notably, Figure 5 also highlights a notable reduction in *A. castellanii* viability compared to the solvent

control, following treatment with pentamidine alone after 24 h of incubation. For GO-CHI-Pent, significant reductions in *A. castellanii* trophozoite viability were observed at test concentrations (Fig. 5), indicating that nanoconjugates of Doxy and Pent exhibit enhanced effects.

Nanoconjugates of doxycycline and pentamidine exhibited significant effects against excystation

These assays are crucial in order to understand the ability of tested compounds against phenotypic transformation of *A. castellanii*. The histogram in Figure 6A showed that the number of viable cells were maximum in the negative and solvent control. However, both compounds (Doxy, Pent) and their respective nanoconjugates decreased the viable trophozoites in a dose dependent manner. For statistical analysis, a $p < 0.05$ was held significant. The histogram showed that the viability of trophozoites were significantly decreased after treatment with GO-CHI-Doxy and Doxy alone. The cell numbers followed the trend of GO-CHI-Doxy< Doxy < GO-CHI < GO at each concentration. Figure 7A also showed that maximum activity was recorded for GO-CHI-Pent and IC_{50} for GO-CHI-Pent is expected around 25 µg/mL, showing that Pent nanoconjugate reveal enhanced efficacy against the transformation of cysts to trophozoites as compared to GO-CHI-Doxy.

Nanoconjugates of doxycycline and pentamidine exhibited significant effects against encystation

Figure 7B showed that the maximum number of cysts were recorded in the negative and solvent control. Both compounds (Doxy, Pent) and their respective nanoconjugates decreased the number of viable cysts with increasing concentrations. The histogram showed that the trend of GO-CHI-Doxy < Doxy < GO-CHI < GO at each concentration. These observations held statistical significance ($p<0.05$). However, only significant activity was recorded for GO-CHI-

Doxy, indicating that only Doxy nanoconjugate showed potent activity against transformation of trophozoites to cysts. Similarly, Figure 7B also highlights that viability of cysts were also reduced after treatment with Pent and its nanoconjugate, in a dose dependent manner. Pent and its' nanoconjugates revealed a notable reduction in cyst viability compared to Doxy and its' nanoconjugates. These results indicate that only Pent and its' nanoconjugates have the ability to inhibit the phenotypic transformation of trophozoites to cysts.

Nano-conjugated Doxy and Pent showed reduced cytotoxicity against HaCaT cells

The cell cytotoxicity assay aimed to assess the cytotoxic effects of drugs and their nano-conjugates on HaCaT cells. As depicted in Figure 6, cytotoxicity decreased with decreasing concentrations of drugs. Specifically, GO-CHI-Doxy exhibited reduced toxicity to human cells compared to Doxy alone. Additionally, the toxicity of GO was mitigated by the addition of chitosan. HaCaT cells displayed low sensitivity to both GO and GO-CHI. The histogram indicates that the highest cytotoxicity was observed for Pent 100µg/mL, reaching up to 41%, followed by Pent alone at lower concentrations. Furthermore, minimal cell cytotoxicity (less than 20%) was observed in HaCaT cells across various concentrations of GO alone as well as GO-CHI.

Discussion

To date, *Acanthamoeba* infections remain difficult to treat (Alawfi et al., 2024). Combination of drugs including amidines, biguanides, and azoles are currently available treatment options with limited efficacy (Elsheikha et al. 2020). In the present study, we used Pent, Doxy and their nanocomposites against *A. castellanii* to assess and compare their anti-amoebic activities. Notably, Doxy exhibited amoebicidal effects in a concentration-dependent pattern. The antimicrobial mechanism of Doxy is correlated to the inhibition of protein synthesis,

which may explain our findings in *A. castellanii*. Doxycycline can inhibit aminoacyl-tRNA (aa-tRNA), which is essential for protein synthesis (Patel and Parmar, 2022). Additionally, Doxy has higher lipophilicity compared to other tetracyclines, allowing it to cross multiple membranes to reach the target site (Patel and Parmar, 2022), making Doxy a promising drug. Furthermore, the viability of *A. castellanii* was also inversely proportional to the concentration of compounds utilized. Both GO and GO-CHI exhibited low amoebicidal effects against *A. castellanii*, likely through interaction with negatively charged membranes (Khandegar et al. 2021).

Pentamidine is one of the well-known drugs that is used to treat *Acanthamoeba* infections, however it lacks specificity and displays toxicity. In this study, we investigated the effects of Pent loaded with its nanomaterials against *A. castellanii* via amoebicidal and cell cytotoxicity assays. The amoebicidal assay results revealed that Pent alone and Pent loaded with its nanoconjugates exhibited anti-amoebic activity against *A. castellanii*. The ability of Pent to inhibit growth is believed to be associated with the hindrance of phospholipids and protein synthesis. The latter can be done via inhibiting the incorporation of nucleic acids into DNA and RNA, as well as blocking the process of oxidative phosphorylation (Fiorito, 2021). Moreover, cell shrinkage and membrane blebbing is one of the key features of cells in late-stage apoptosis, and it can be seen in *A. castellanii* trophozoites upon exposure to pentamidine (Baig et al., 2017). Thus, the amoebicidal effects exhibited by Pent alone may be due apoptosis-inducing properties, eventually leading to cell death in *Acanthamoeba*. Microbial cell membranes can be intruded by the sharp edges of GO, leading to consequent cytoplasmic content leakage and therefore inducing cell death (Mohammed et al, 2020; Radhi et al., (2021). Oxidative stress is also attributed to the formation of lipid peroxide by reactive oxygen species (ROS) which causes the oxidation of fatty acid. The physicochemical property of GO which generates ROS leads to

damage of DNA and RNA. Furthermore, GO-CHI showed more activity against *A. castellanii* trophozoites as compared to GO. This could be due to the fact that antimicrobial properties are also exhibited with the conjugation of graphene oxide and chitosan. The increase in killing action may be associated with the increase in roughness of GO-CHI surface (Sundar et al., 2014). Most importantly, the synergistic effect between graphene oxide and chitosan may allow the enhancement of anti-acanthamoebic effects against *A. castellanii*. Besides, the number of viable *A. castellanii* trophozoites significantly decreased after treatment with GO-CHI-Pent at 100µg/mL. This decreased activity is possibly due to the use of nano-conjugates, while GO-CHI serves as a drug carrier. Owing to the efficient encapsulation efficiency of graphene oxide and chitosan (Khandegar et al., 2021), it is likely that the loaded Pent drug does not leak out before reaching the targeted cell and inhibiting the incorporation of DNA and RNA resulting in cell death (Grumezescu, 2019). Kumar et al. (2021) suggest that the extended release of Metronidazole, which is an antifungal drug, is observed when using GO-CHI to carry the drug. We also propose that Pent which is also an antifungal drug will have extended drug release when conjugated with GO-CHI. With the administration of higher concentrations of GO-CHI-Pent, higher cytotoxicity can be seen (Figure 6), resulting from the higher drug concentration that correlates to its cytotoxicity. Bellmann and Smuszkiewicz, (2017) reported that amphotericin B is analogous to Pent, and demonstrated a direct proportional relationship between the drug concentration and its toxicity, which further supported the aforementioned concept. However, when compared with pentamidine alone, cytotoxicity was reduced upon conjugation with GO-CHI. Similarly, Doxy showed moderate cytotoxicity by itself, whereas the nano-conjugated GO-CHI-Doxy exhibited the lowest toxicity. This indicates that the use of GO-CHI nanoconjugates as a drug carrier for Pent and Doxy attenuates the cytotoxic effects of drugs alone as also

reported previously (Shu et al., 2021). These nanomaterials especially GO-CHI-Doxy revealed potent anti-amoebic activities and limited cytotoxicity *in vitro*.

The phenotypic transformation assessment into the nanomaterials, along with their respective controls, was also performed to explore their potential inhibitory effects against *A. castellanii*. These assays are critical as hash environments, chemicals and drugs lead to the transformation of trophozoites to cysts, making infections difficult to eradicate (Ahmed et al., 2022). These GO and GO-Chi have previously shown potent anticancer and anti-microbial effects (Bhatti et al., 2018; Ma et al., 2022) and their combination with Dox and Pent significantly inhibited excystation and encystation of *A. castellanii*. These enhanced effects may be due to synergistic effect of both GO-Chi and drugs, providing a dual mode of action. Based on the data from our study, these nanomaterials should be considered for future *in vivo* studies for *Acanthamoeba* infections, eventually being considered to develop effective contact lens cleaning solutions.

In conclusion, GO-CHI-Doxy and GO-CHI-Pent exhibited significantly stronger amoebicidal effects against *A. castellanii* in comparison to drugs alone. These nanoconjugates may have potential against *Acanthamoeba* keratitis and encephalitis, however *in vivo* studies are needed to realize these expectations. Furthermore, GO-CHI-Doxy showed lower cytotoxicity against human cells. GO-CHI-Pent decreased the viability of *A. castellanii but* showed relatively higher cytotoxicity. Future mechanistic studies are warranted to understand the mechanism of action of drugs with their nano-conjugates.

Acknowledgement

This research work was supported by Sunway University, Malaysia, and University of Karachi, Pakistan.

Authors contributions

TB and JG synthesized and characterized the materials under the supervision of MRS. UA, MD, BSA, AA, TYY, YJT planned and performed all assays and carried out the work under the supervision of NAK and MRS. TJ, UA and UA drafted the manuscript. MRS, NAK, RS and AA corrected and finalized the manuscript. MRS and AA conceived the idea and acquired funding. All authors approved the manuscript.

Funding

This research work was supported by Sunway University, Malaysia GRTIN-RRO-46-2022. Ruqaiyyah Siddiqui and Naveed Ahmed Khan are supported by the Air Force Office of Scientific Research (AFOSR), USA.

Competing interest

The authors declare that they have no competing interest.

Ethical approval

Not required.

Data availability

Data will be provided upon request on case-to-case basis.

Clinical trial number: Not applicable.

References

462 Ahmed U, Manzoor M, Qureshi S, Mazhar M, Fatima A, Aurangzeb S, Hamid M, Khan KM, Khan
463 NA, Rashid Y, Anwar A (2023a) Anti-amoebic effects of synthetic acridine-9 (10*H*)-one
464 against brain-eating amoebae. Acta Trop. 106824.

465 Ahmed U, Ong SK, Khan KM, Siddiqui R, Khan NA, Shaikh MF, Alawfi BS, Anwar A (2023b)
466 Effect of embelin on inhibition of cell growth and induction of apoptosis in *Acanthamoeba*
467 *castellanii*. Arch Microbiol. 205(12). 360.

468 Alawfi BS, Khan NA, Lloyd D, Siddiqui R (2024) *Acanthamoeba* keratitis: new hopes for potential
469 interventions for a curable but often refractory disease. Exp. Rev. Ophthalmol. 19(4): 271-
470 280.

471 Alizadeh H, Silvany RE, Meyer DR, Dougherty JM, McCulley JP (1997) In vitro amoebicidal
472 activity of propamidine and pentamidine isethionate against *Acanthamoeba* species and
473 toxicity to corneal tissues. Cornea. 16(1):94-100.

474 Anwar A, Khan NA, Siddiqui R (2018) Combating *Acanthamoeba* spp. cysts: what are the
475 options?. Parasit. Vectors. 11(1):1-6.

476 Anwar A, Chi Fung L, Anwar A, Jagadish P, Numan A, Khalid M, Shahabuddin S, Siddiqui R,
477 Khan NA (2019a) Effects of shape and size of cobalt phosphate nanoparticles against
478 *Acanthamoeba castellanii*. Pathogens. 8(4):260.

479 Anwar A, Mungroo MR, Anwar A, Sullivan Jr WJ, Khan NA, Siddiqui R (2019b) Repositioning
480 of guanabenz in conjugation with gold and silver nanoparticles against pathogenic amoebae
481 *Acanthamoeba castellanii* and *Naegleria fowleri*. ACS Infect. Dis. 5(12):2039-46.

Azizan NF, Yusof H (2021) Distribution of *Acanthamoeba* genotypes isolated from recreational water resources: a review. Science, Engineering and Health Studies, 15, 21010002.Baig AM, Lalani S, Khan NA (2017) Apoptosis in *Acanthamoeba castellanii* belonging to the T4 genotype. J. Basic Microbiol. 57(7):574-9.

Bellmann R, Smuszkiewicz P (2017) Pharmacokinetics of antifungal drugs: practical implications for optimized treatment of patients. Infection. 45:737-79. Biswas K, Janani G, Udayakumar S, Deepika B, Girigoswami K (2023). Rough edges of reduced graphene oxide (rGO) sheets elicit anticancerous activities: An in vitro study. Results in Chemistry. 6:101207.

Keerthana V, Girigoswami A, Jothika S, Kavitha D, Gopikrishna A, Somanathan T, Girigoswami K. (2022). Synthesis, characterization and applications of GO–TiO2 nanocomposites in textile dye remediation. Iranian Journal of Science and Technology, Transactions A: Science. 46(4):1149-61.

Cheng MM, Huang LJ, Wang YX, Zhao YC, Tang JG, Wang Y, Zhang Y, Hedayati M, Kipper MJ, Wickramasinghe SR (2019) Synthesis of graphene oxide/polyacrylamide composite membranes for organic dyes/water separation in water purification. J. Mater. Sci. 54(1):252-64.

Chiu NF, Chen CC, Yang CD, Kao YS, Wu WR (2018) Enhanced plasmonic biosensors of hybrid gold nanoparticle-graphene oxide-based label-free immunoassay. Nanoscale Res. Lett. 13(1):1-1.

Clarke, D.W., Niederkorn, J.Y., 1999. The pathophysiology of *Acanthamoeba* keratitis. Trends Parasitol. 22, 175-180.

503 Deb A, Vimala R. (2018) Natural and synthetic polymer for graphene oxide mediated anticancer
504 drug delivery—A comparative study. Int. J. Biol. Macromol. 107:2320-33.

505 Debnath A (2021) Drug discovery for primary amebic meningoencephalitis: from screen to
506 identification of leads. Exp. Rev. Anti-Infect. Ther. 19(9):1099-1106.

507 Deng S, Berry V (2016) Wrinkled, rippled and crumpled graphene: an overview of formation
508 mechanism, electronic properties, and applications. Mater. Today. 19(4):197-212.

509 Diehl ML, Paes J, Rott MB (2021) Genotype distribution of *Acanthamoeba* in keratitis: a
510 systematic review. Parasitol. Res. 120:3051-63.

511 El Rouby WM, Farghali AA, Sadek MA, Khalil WF (2018) Fast removal of Sr (II) from water by
512 graphene oxide and chitosan modified graphene oxide. J. Inorg. Organomet. Polym. Mater.
513 28:2336-49.

514 Elsheikha HM, Siddiqui R, Khan NA (2020) Drug discovery against *Acanthamoeba* infections:
515 Present knowledge and unmet needs. Pathogens. 9(5):405. 1(1):8053.

516 Feng W, Wang Z (2022) Biomedical applications of chitosan-graphene oxide nanocomposites.
517 Iscience. 25(1):103629.

518 Gong Y, Yu Y, Kang H, Chen X, Liu H, Zhang Y, Sun Y, Song H (2019) Synthesis and
519 Characterization of Graphene Oxide/Chitosan Composite Aerogels with High Mechanical
520 Performance. Polymers 11(5):777.

521 Grumezescu, A. M. (2019). Nanomaterials for Drug Delivery and Therapy. Elsevier, Amsterdam,
522 Nethrrlands, pp551. ISBN: 9780128165058.

Henriquez FL, Mooney R, Bandel T, Giammarini E, Zeroual M, Fiori PL, Margarita V, Rappelli P, Dessì D (2021) Paradigms of protist/bacteria symbioses affecting human health: *Acanthamoeba* species and *Trichomonas vaginalis*. Front. Microbiol. 11:e616213.

Jeyamogan S, Khan NA, Anwar A, Shah MR, Siddiqui R (2018) Cytotoxic effects of Benzodioxane, Naphthalene diimide, Porphyrin and Acetamol derivatives on HeLa cells. SAGE Open Med. 6:2050312118781962.

Jha BK, Seo I, Kong HH, Suh SI, Suh MH, Baek WK (2015) Tigecycline inhibits proliferation of *Acanthamoeba castellanii*. Parasitol. Res. 114:1189-1195.

Kannan S, Harel Y, Israel LL, Lellouche E, Varvak A, Tsubery MN, Lellouche JP, Michaeli S (2021) Novel Nanocarrier Platform for Effective Treatment of Visceral Leishmaniasis. Bioconjugate Chem. 32(11):2327-41.

Kesavan S, Meena KS, Sharmili SA, Govindarajan M, Alharbi NS, Kadaikunnan S, Khaled JM, Alobaidi AS, Alanzi KF, Vaseeharan B (2021) Ulvan loaded graphene oxide nanoparticle fabricated with chitosan and d-mannose for targeted anticancer drug delivery. J. Drug Deliv. Sci. Technol. 65:102760.

Khan, N.A., 2006. *Acanthamoeba*: biology and increasing importance in human health. FEMS Microbiol. Rev. 30, 564-595.

Khandegar V, Kaur PJ, Chanana P (2021) Chitosan and Graphene Oxide-based Nanocomposites for Water Purification and Medical Applications: A Review. BioResources. 16(4):8525-66.

543 Kumar G, Chaudhary K, Mogha NK, Kant A, Masram DT (2021) Extended release of
544 metronidazole drug using chitosan/graphene oxide bionanocomposite beads as the drug
545 carrier. ACS Omega. 6(31):20433-44.

546 Kumar S, Koh J (2014) Physiochemical and optical properties of chitosan based graphene oxide
547 bionanocomposite. Int. J. Biol. Macromol. 70:559-64.

548 Lamien-Meda A, Köhsler M, Walochnik J (2022) Real-Time PCR for the Diagnosis of
549 *Acanthamoeba* Genotype T4. Microorganisms. 10(7):1307.

550 Han D, Yan L, Chen W, Li W (2011) Preparation of chitosan/graphene oxide composite film with
551 enhanced mechanical strength in the wet state. Carbohyd. Poly. 83(2): 653-658.

552 Malek AE, Granwehr BP, Kontoyiannis DP (2020) Doxycycline as a potential partner of COVID-
553 19 therapies. IDCases. 21:e00864.

554 Mannis MJ, and Holland EJ (2021) Cornea, 2-volume set (Fifth). Elsevier. Book ISBN:
555 9780323674720.

556 Manzoor AA, Lindner LH, Landon CD, Park JY, Simnick AJ, Dreher MR, Das S, Hanna G, Park
557 W, Chilkoti A, Koning GA (2012) Overcoming limitations in nanoparticle drug delivery:
558 triggered, intravascular release to improve drug penetration into tumors. Cancer Res.
559 72(21):5566-75.

560 Marciano-Cabral, F., Cabral, G., 2003. *Acanthamoeba* spp. as agents of disease in humans. Clin.
561 Microbiol. Rev. 16, 273-307.

562 Mohammed H, Kumar A, Bekyarova E, Al-Hadeethi Y, Zhang X, Chen M, Ansari MS, Cochis A,
563 Rimondini L (2020) Antimicrobial mechanisms and effectiveness of graphene and
564 graphene-functionalized biomaterials. A scope review. Front. Bioeng. Biotechnol. 8:465.

565 Motiei M, Kashanian S (2017) Novel amphiphilic chitosan nanocarriers for sustained oral delivery
566 of hydrophobic drugs. Eur. J. Pharm. Sci. 99:285-91.

567 Marcano DC, Kosynkin DV, Berlin JM, Sinitskii A, Sun Z (2010) Improved Synthesis of
568 Graphene oxide. ACS Nano 4(8): 4806-4814.

569 Narendrakumar L, Joseph I, Thomas S (2021) Potential effectiveness and adverse implications of
570 repurposing doxycycline in COVID-19 treatment. Expert Rev. Anti-infect. Ther.
571 19(8):1001-8.

572 Ong TYY, Khan NA, Siddiqui R (2017) Brain-eating amoebae: predilection sites in the brain and
573 disease outcome. J. Clin. Microbiol. 55(7):1989-1997.

574 Panjwani, N., 2010. Pathogenesis of *Acanthamoeba* keratitis. Ocul. Surf. 8, 70-79.

575 Patel RS, Parmar M (2022) Doxycycline Hyclate. In: StatPearls. StatPearls Publishing, Treasure
576 Island (FL); 2022. PMID: 32310348.

577 Peretti E, Miletto I, Stella B, Rocco F, Berlier G, Arpicco S (2018) Strategies to obtain
578 encapsulation and controlled release of pentamidine in mesoporous silica nanoparticles.
579 Pharmaceutics. 10(4):195.

580 Radhi A, Mohamad D, Rahman FS, Abdullah AM, Hasan H (2021) Mechanism and factors
581 influence of graphene-based nanomaterials antimicrobial activities and application in
582 dentistry. J. Mater. Res. Technol. 11:1290-307.

583 Rana VK, Choi MC, Kong JY, Kim GY, Kim MJ, Kim SH, Mishra S, Singh RP, Ha CS (2011)
584 Synthesis and drug-delivery behavior of chitosan-functionalized graphene oxide hybrid
585 nanosheets. Macromol. Mater. Eng. 296(2):131-40.

586 Rayamajhee B, Willcox M, Sharma S, Mooney R, Petsoglou C, Badenoch PR, Sherchan S,
587 Henriquez FL, Carnt N (2024) Zooming in on the intracellular microbiome composition of
588 bacterivorous *Acanthamoeba* isolates. ISME Comm. 4(1):e016.

589 Reyes-Batlle M, Sifaoui I, Rodríguez-Expósito RL, Piñero JE, Lorenzo-Morales J (2022) New
590 Insights in *Acanthamoeba*. Pathogens. 11(5):609.

591 Safdar M, Ozaslan M, Junejo Y (2021) Synthesis, characterization and employed doxycycline
592 capped gold nanoparticles on TRP channel expressions in SKBR3 breast cancer cells and
593 antimicrobial activity. J. Clust. Sci. 33(6) 635-2642.

594 Sanderson L, Da Silva M, Sekhar GN, Brown RC, Burrell-Saward H, Fidanboylu M, Liu B, Dailey
595 LA, Dreiss CA, Lorenz C, Christie M (2021) Drug reformulation for a neglected disease.
596 The NANOHAT project to develop a safer more effective sleeping sickness drug. PLoS
597 Negl. Trop. Dis. 15(4):e0009276.

598 Sangkanu S, Mitsuwan W, Mahabusarakam W, Jimoh TO, Wilairatana P, Girol AP, Verma AK,
599 de Lourdes Pereira M, Rahmatullah M, Wiart C, Siyadatpanah A (2021) Anti-
600 Acanthamoeba synergistic effect of chlorhexidine and Garcinia mangostana extract or α-
601 mangostin against *Acanthamoeba triangularis* trophozoite and cyst forms. Sci. Rep.
602 11(1):8053.

603 Saravanabhavan SS, Rethinasabapathy M, Zsolt S, Kalambettu AB, Elumalai S, Janakiraman M,
604 Huh YS, Natesan B (2019) Graphene oxide functionalized with chitosan based

nanoparticles as a carrier of siRNA in regulating Bcl-2 expression on Saos-2 & MG-63 cancer cells and its inflammatory response on bone marrow derived cells from mice. Mater. Sci. Eng. C Mater. Biol. Appl. 99:1459-1468.

Shanmuga SS, Natarajan K, Zsolt S, Priya LS, Ayyar M, Anboo S, Nissapatorn V, Jonna N, Vasanthapalaniappan K, Packirisamy R, Dolma KG (2024) In vitro study on the inflammatory response of chitosan nanoparticles as a potential siRNA carrier targeting towards osteosarcoma cells. Zeitschrift für Physikalische Chemie. 238(7): 1345-1360.

Shahriary L, Athawale AA (2014) Graphene oxide synthesized by using modified hummers approach. Int. J. Renew. Energy Environ. Eng. 2(01):58-63.

Shu M, Gao F, Zeng M, Yu C, Wang X, Huang R, Yang J, Su Y, Hu N, Zhou Z, Liu K (2021) Microwave-assisted chitosan-functionalized graphene oxide as controlled intracellular drug delivery nanosystem for synergistic antitumour activity. Nanoscale Res. Lett. 16(1):75.

Siddiqui R, Aqeel Y, Khan NA (2016) The development of drugs against *Acanthamoeba* infections. Antimicrob. Agents Chemother. 60(11):6441-50.

Singh G, Nenavathu BP (2020) Development of rGO encapsulated polymeric beads as drug delivery system for improved loading and controlled release of doxycycline drug. Drug Dev. Ind. Pharm. 46(3):462-70.

Su Z, Sun D, Zhang L, He M, Jiang Y, Millar B, Douglas P, Mariotti D, Maguire P, Sun D (2021) Chitosan/silver nanoparticle/graphene oxide nanocomposites with multi-drug release, antimicrobial, and photothermal conversion functions. Materials. 14(9):2351.

626 Sundar K, Harikarthick V, Karthika VS, Ravindran A (2014) Preparation of chitosan-graphene
627 oxide nanocomposite and evaluation of its antimicrobial activity. J. Bionanosci. 8(3):207-
628 12.

629 Turner, N.A., Russell, A.D., Furr, J.R., Lloyd, D., 2004. Resistance, biguanide sorption and
630 biguanide-induced pentose leakage during encystment of *Acanthamoeba castellanii*. J.
631 Appl. Microbiol. 96, 1287-1295.

632 Veerapandian M, Neethirajan S (2015) Graphene oxide chemically decorated with Ag–
633 Ru/chitosan nanoparticles: fabrication, electrode processing and immunosensing
634 properties. RSC Adv. 5(92):75015-24.

635 Visvesvara, G.S., Moura, H., Schuster, F.L., 2007. Pathogenic and opportunistic free-living
636 amoebae: *Acanthamoeba* spp., *Balamuthia mandrillaris*, *Naegleria fowleri*, and *Sappinia*
637 *diploidea*. FEMS Immunol. Med. Microbiol. 50, 1-26.

638 Wang W, Xue C, Mao X (2020) Chitosan: Structural modification, biological activity and
639 application. Int. J. Biol. Macromol. 164:4532-4546.

640 Yadav M, Parle M, Sharma N, Dhingra S, Raina N, Jindal DK (2017) Brain targeted oral delivery
641 of doxycycline hydrochloride encapsulated Tween 80 coated chitosan nanoparticles
642 against ketamine induced psychosis: behavioral, biochemical, neurochemical and
643 histological alterations in mice. Drug Deliv. 24(1):1429-40.

644 Ma J, Liu Y, Chen M, Li M, Xu S, Liu H (2022) Dual-sensitive GO-based self-assembly for the
645 delivery of a hydrophobic anti-cancer drug. N J Chem. 46(45):21942-9.

646 Bhatti HT, Ahmad NM, Khan Niazi MB, Ur Rehman Alvi MA, Ahmad N, Anwar MN, Cheema
647 W, Tariq S, Batool M, Aman Z, Janjua HA (2018) Graphene Oxide-PES-Based Mixed

Matrix Membranes for Controllable Antibacterial Activity against Salmonella typhi and Water Treatment. Int J Polym Sci. 2018(1):7842148.

Ahmed U, Anwar A, Ong SK, Anwar A, Khan NA (2022) Applications of medicinal chemistry for drug discovery against *Acanthamoeba* infections. Med Res Rev. 42(1):462-512.

Figure legends:

Figure 1: Representative FTIR spectra for the prepared (a) GO, GO-CHI, CHI (b) GO-CHI, GO-CHI-Doxy, Doxy(c) GO-CHI, GO-CHI-Pent, Pent.

Figure 2: Thermogravimetric analysis of GO, CHI and Functionalized GO-CHI.

Figure 3: Representative (i) AFM and (ii) SEM micrographs of (A) GO, (B) GO-CHI, (C) GO-CHI-Doxy and (D) GO-CHI-Pent.

Figure 4: X-Ray Diffractograms of GO, CHI and GO-CHI.

Figure 5: Illustrated the number of viable *A. castellanii* trophozoites after 24-hour incubation with various concentrations of GO, GO-Chi, Doxy, GO-Chi/Doxy, Pent, and GO-Chi/Pent. Chlorhexidine (100 µg/mL) was used as a positive control, while ddH_2O was used as a solvent control.

Figure 6: (a) Illustrated the cytotoxicity effects of GO, GO-Chi, Doxy, Pent, GO-Chi/Doxy and GO-Chi/Pent against HaCaT cells treated with different concentrations of compounds at 37°C after 24-hour incubation.

Figure 7: Illustrate the effect of chitosan-functionalized graphene oxide loaded with doxycycline and pentamidine on the phenotypic transformation. (A) Shows the effect of GO, GO-Chi, Doxy, Pent, GO-Chi/Doxy and GO-Chi/Pent on the excystation of *A. castellanii* cysts to trophozoites after 72-hours of treatment. (B) Demonstrate the effect of GO, GO-Chi, Doxy, Pent, GO-Chi/Doxy and GO-Chi/Pent on the encystment of *A. castellanii* trophozoites to cysts after 72-hours of treatment. Asterisks ('*') indicate that the values are significant, with a *p* value of less than 0.05.

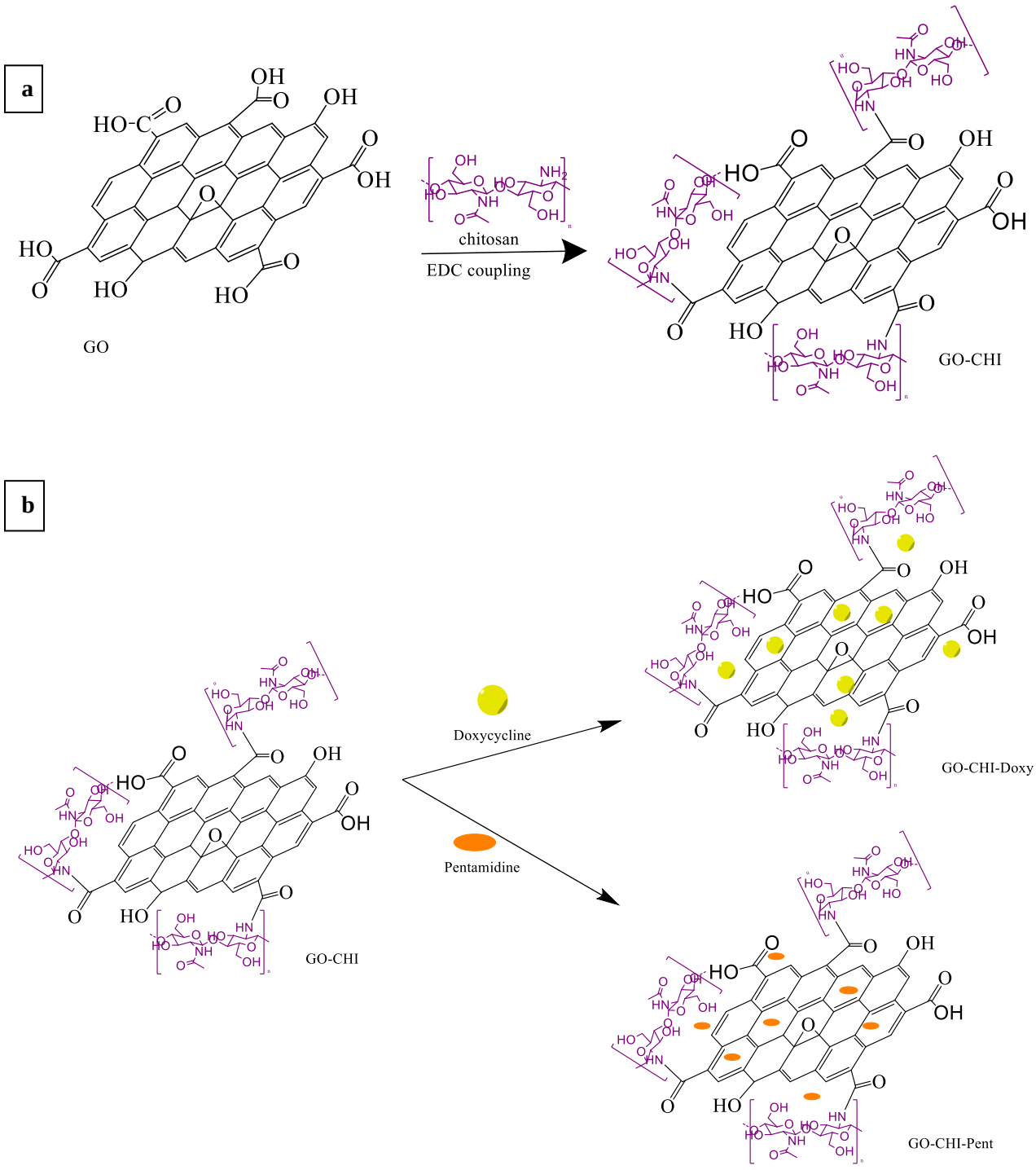
a
GO
chitosan
EDC coupling
GO-CHI
b
GO-CHI
Doxycycline
Pentamidine
GO-CHI-Doxy
GO-CHI-Pent

Fig. 1

a)

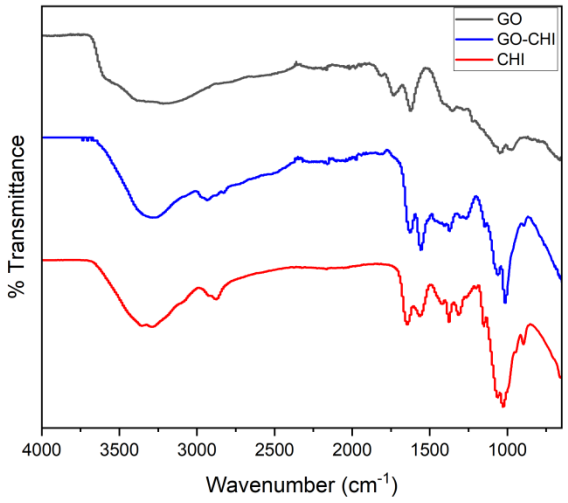
GO
GO-CHI
CHI
% Transmittance
4000
3500
3000
2500
2000
1500
1000
Wavenumber (cm-1)

b)

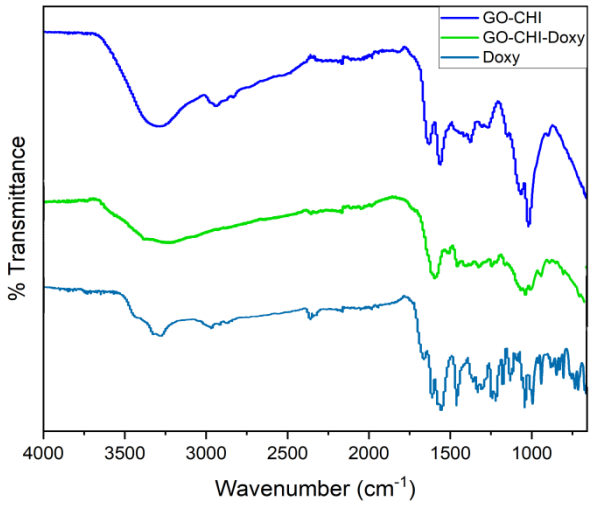
GO-CHI
GO-CHI-Doxy
Doxy
% Transmittance
4000
3500
3000
2500
2000
1500
1000
Wavenumber (cm-1)

c)

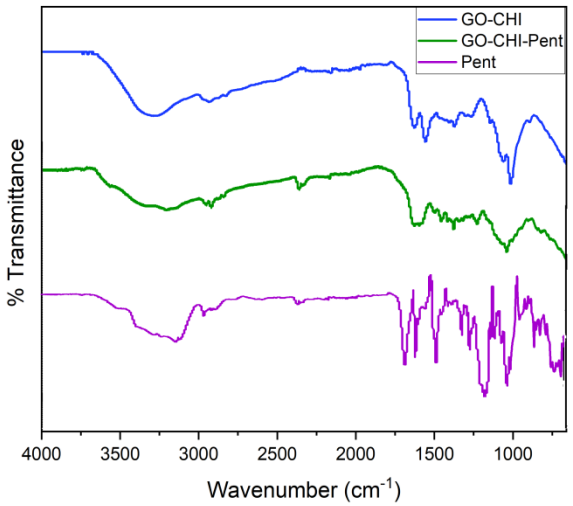
GO-CHI
GO-CHI-Pent
Pent
% Transmittance
4000
3500
3000
2500
2000
1500
1000
Wavenumber (cm-1)

Fig. 2

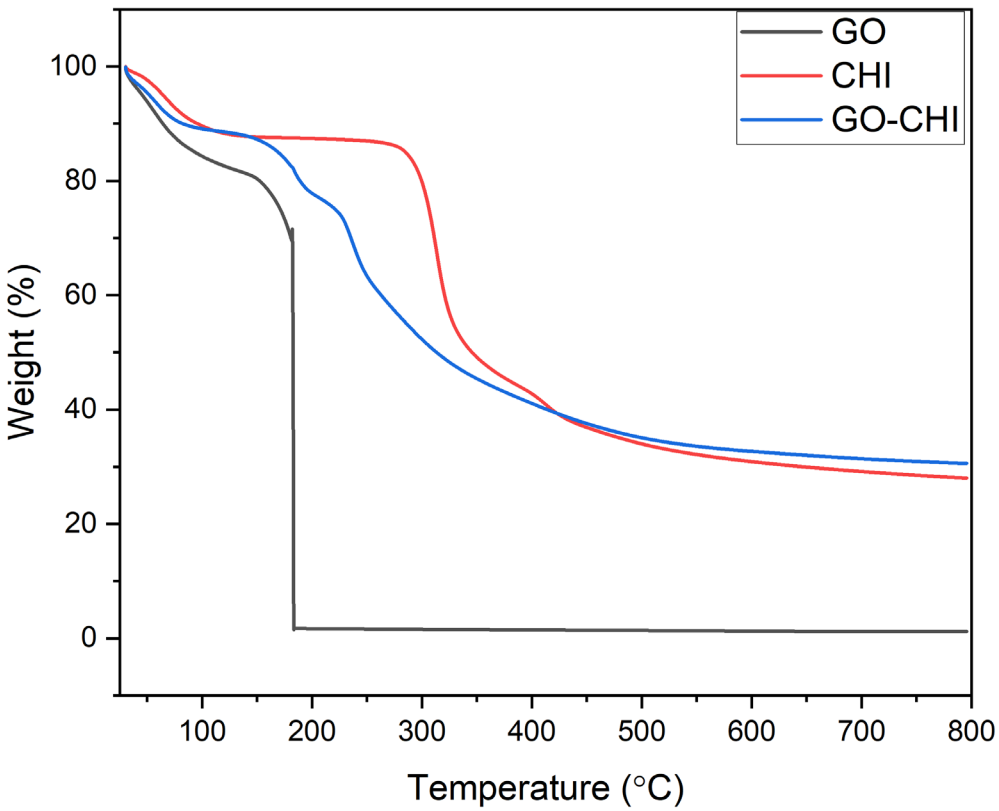
GO
CHI
GO-CHI
Weight (%)
100
80
60
40
20
0
100
200
300
400
500
600
700
800
Temperature (°C)

Fig. 3

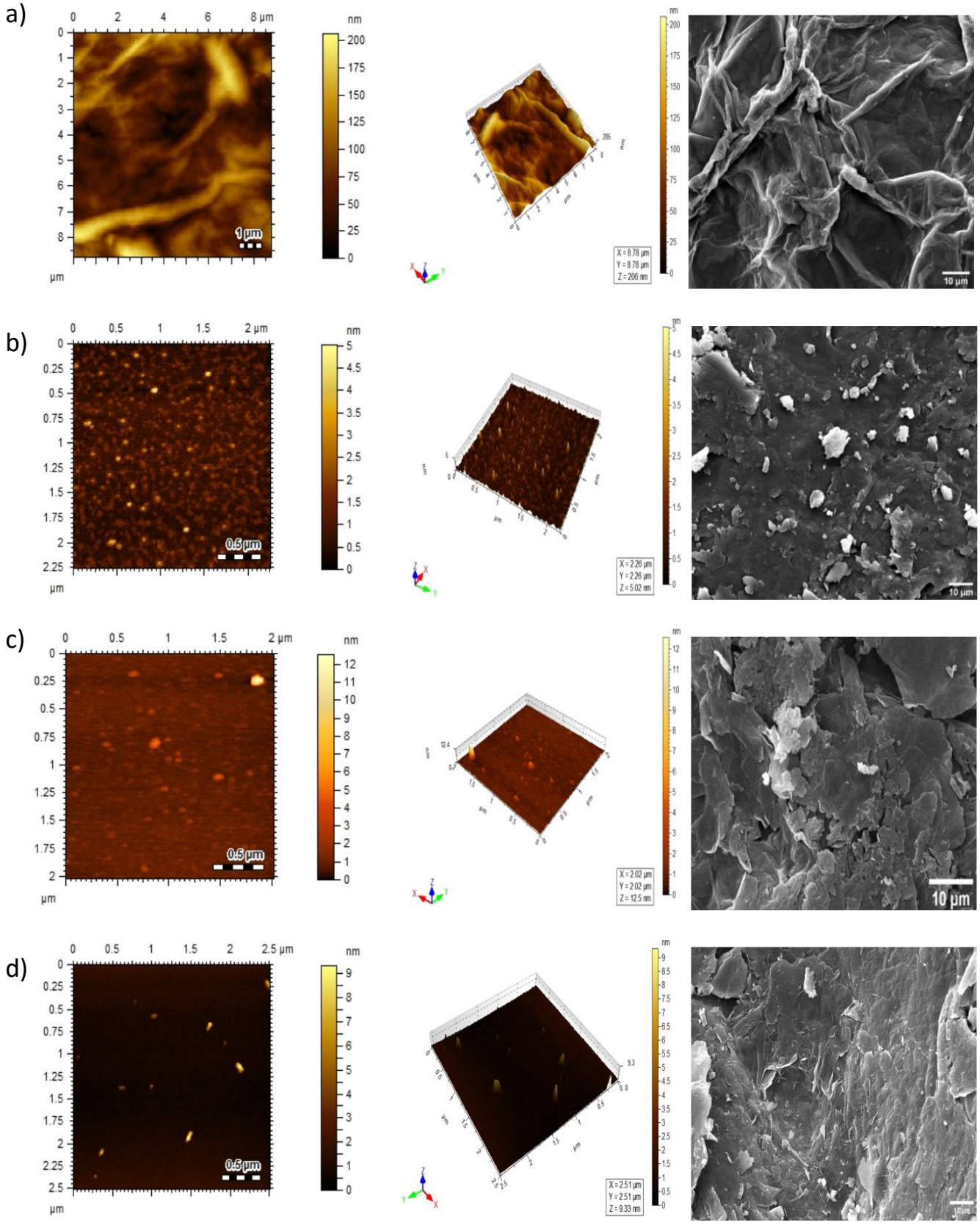

Fig. 4

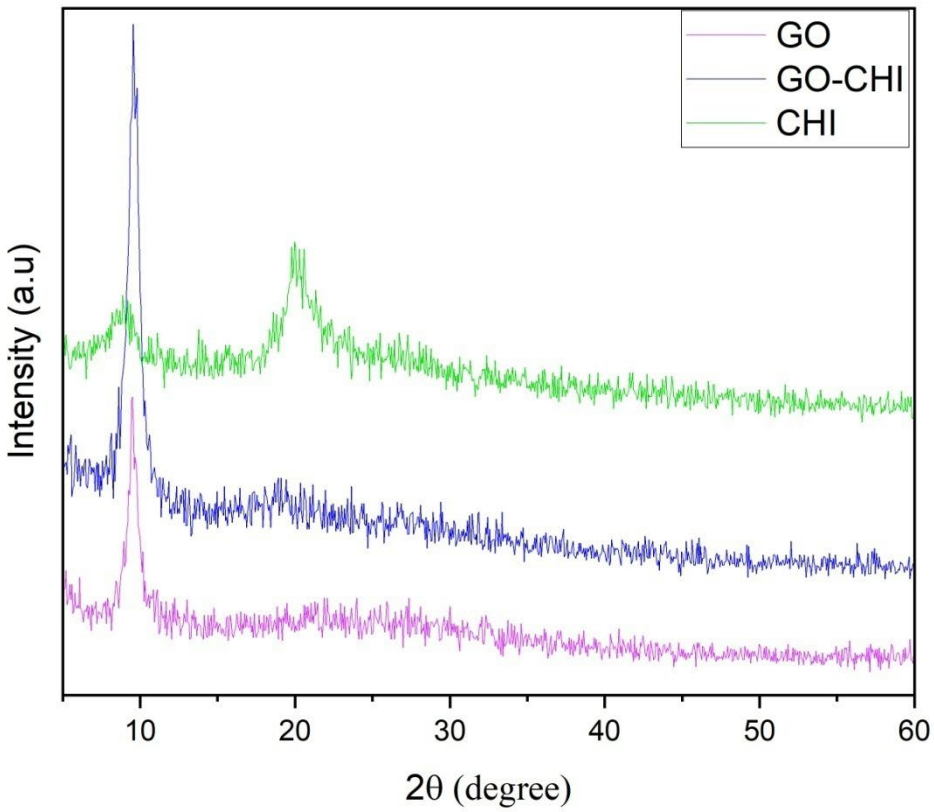

Fig. 5

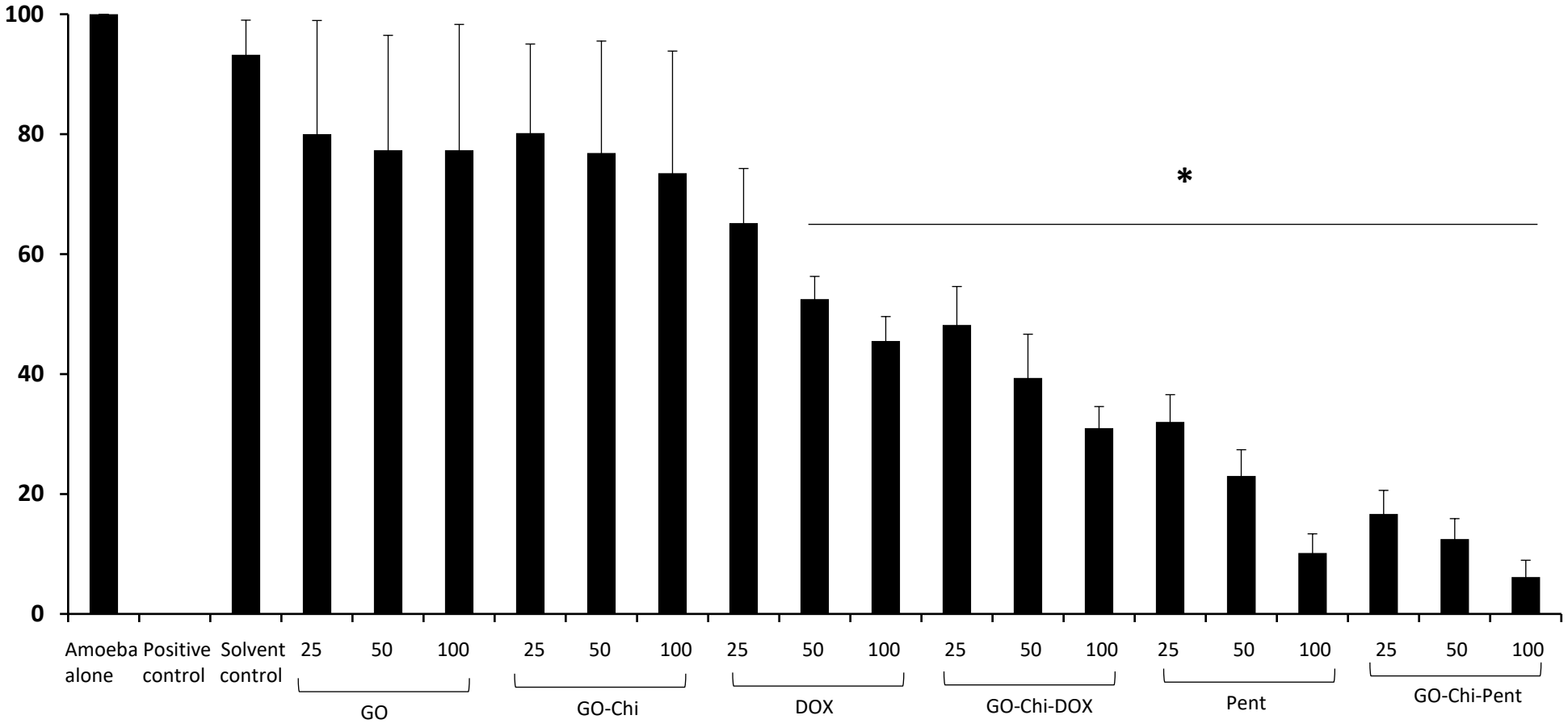
100
80
60
40
20
0
*
Amoeba alone
Positive control
Solvent control
25
50
100
25
50
100
25
50
100
25
50
100
25
50
100
25
50
100
GO
GO-Chi
DOX
GO-Chi-DOX
Pent
GO-Chi-Pent

Fig. 6

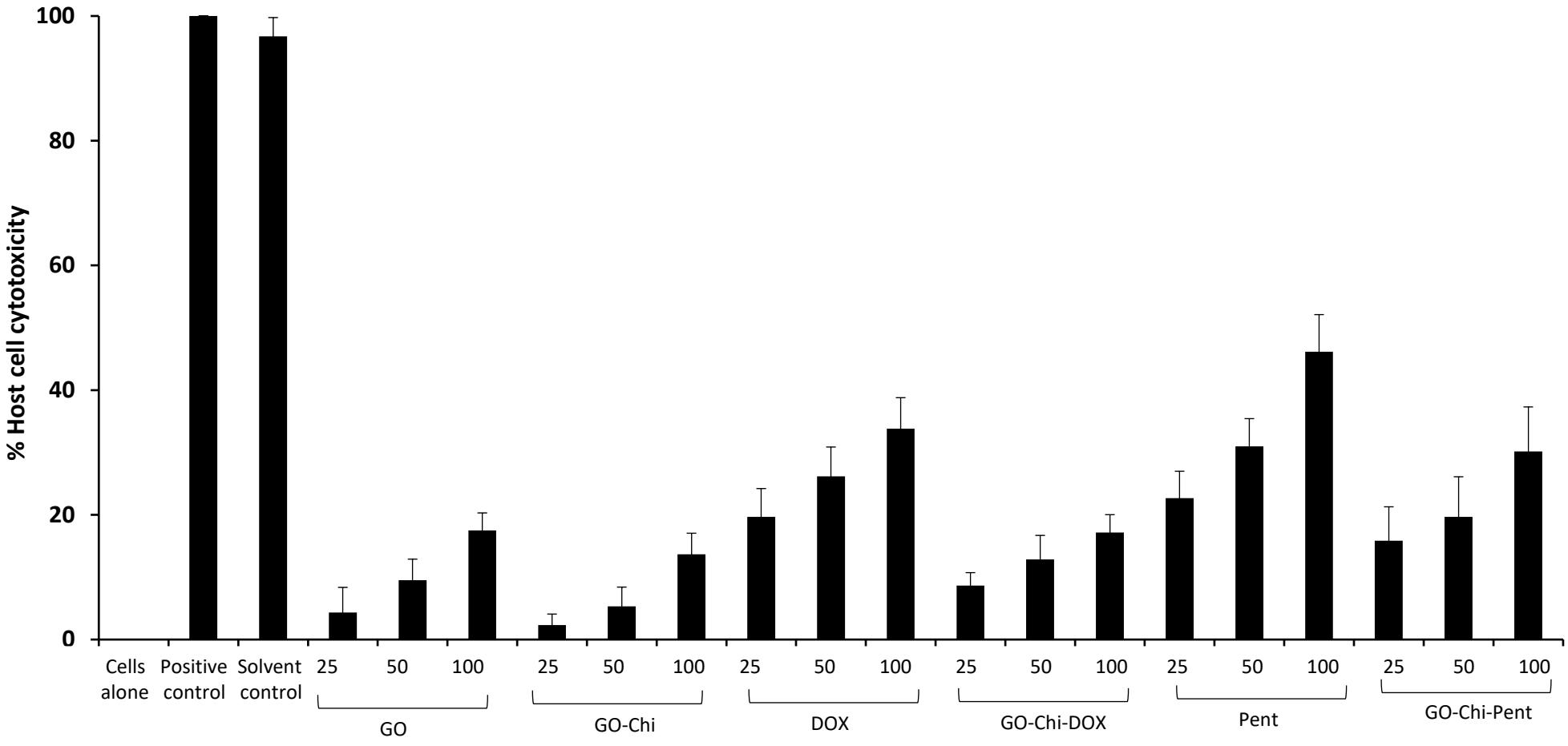
% Host cell cytotoxicity
100
80
60
40
20
0
Cells alone
Positive control
Solvent control
25
50
100
GO
GO-Chi
DOX
GO-Chi-DOX
Pent
GO-Chi-Pent

A

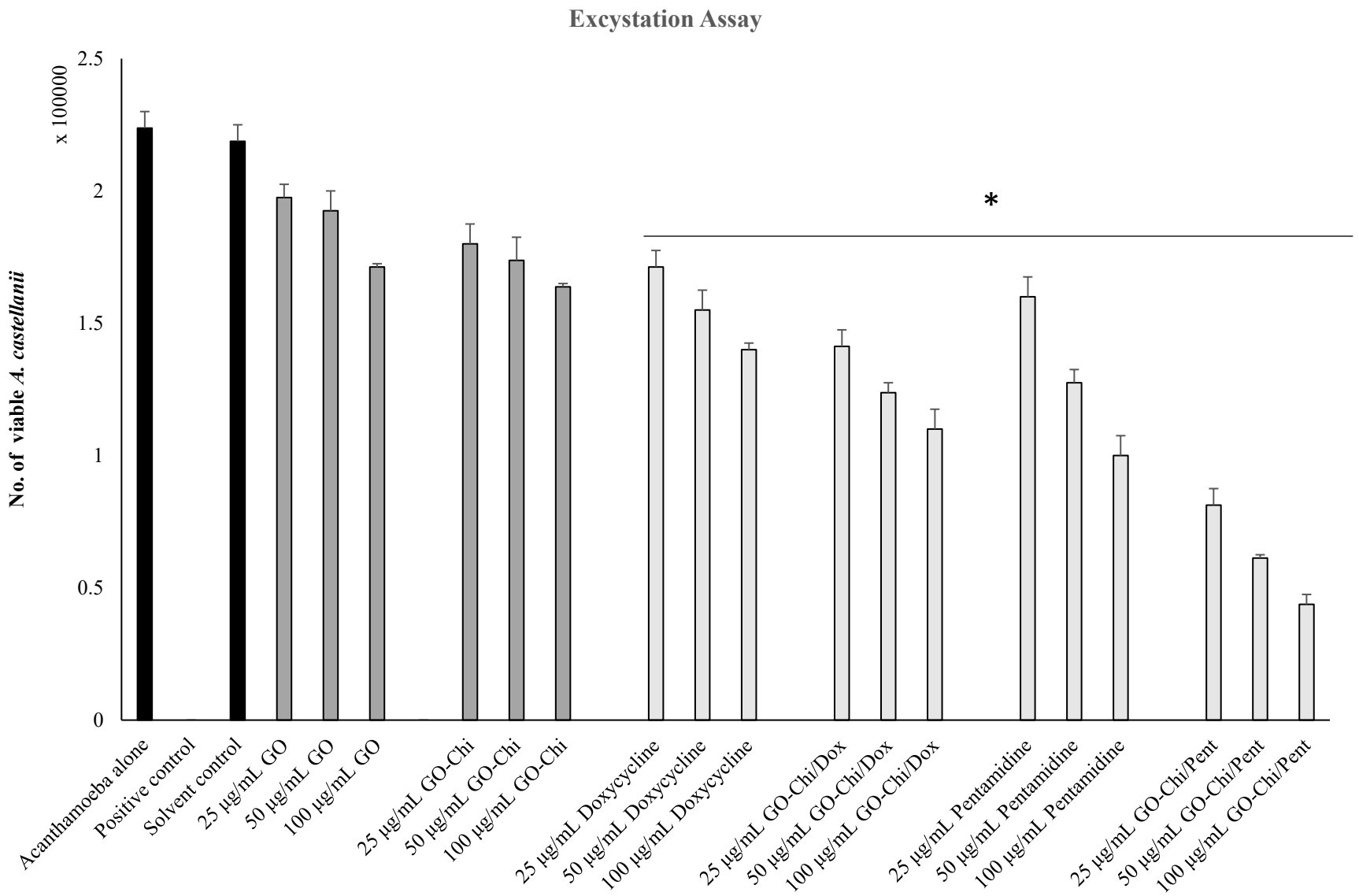
Excystation Assay
No. of viable A. castellanii
x 100000
2.5
2
1.5
1
0.5
0
*
Acanthamoeba alone
Positive control
Solvent control
25 µg/mL GO
50 µg/mL GO
100 µg/mL GO
25 µg/mL GO-Chi
50 µg/mL GO-Chi
100 µg/mL GO-Chi
25 µg/mL Doxycycline
50 µg/mL Doxycycline
100 µg/mL Doxycycline
25 µg/mL GO-Chi/Dox
50 µg/mL GO-Chi/Dox
100 µg/mL GO-Chi/Dox
25 µg/mL Pentamidine
50 µg/mL Pentamidine
100 µg/mL Pentamidine
25 µg/mL GO-Chi/Pent
50 µg/mL GO-Chi/Pent
100 µg/mL GO-Chi/Pent

B

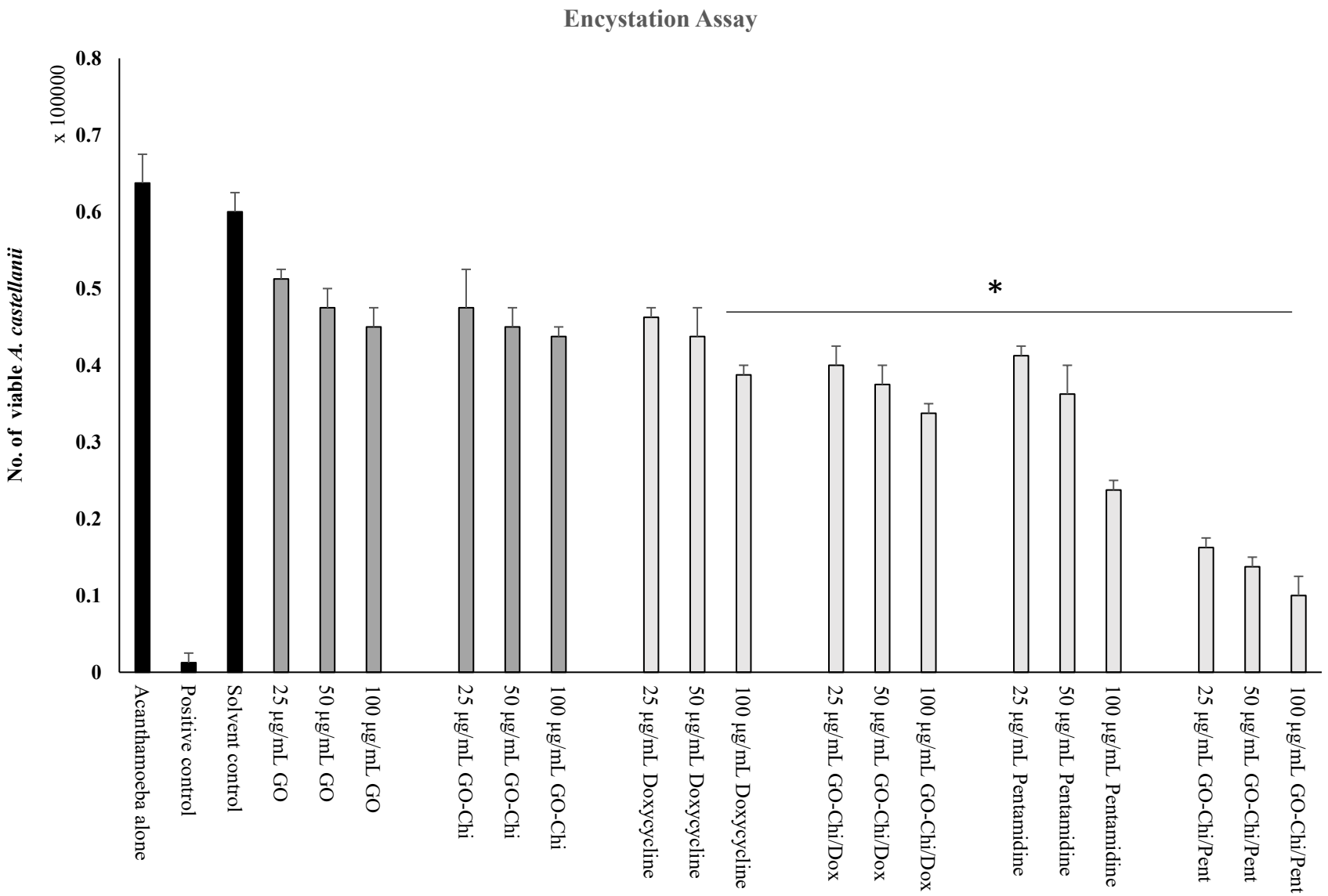
Encystation Assay
No. of viable A. castellanii
x 100000
0.8
0.7
0.6
0.5
0.4
0.3
0.2
0.1
0
*
Acanthamoeba alone
Positive control
Solvent control
25 µg/mL GO
50 µg/mL GO
100 µg/mL GO
25 µg/mL GO-Chi
50 µg/mL GO-Chi
100 µg/mL GO-Chi
25 µg/mL Doxycycline
50 µg/mL Doxycycline
100 µg/mL Doxycycline
25 µg/mL GO-Chi/Dox
50 µg/mL GO-Chi/Dox
100 µg/mL GO-Chi/Dox
25 µg/mL Pentamidine
50 µg/mL Pentamidine
100 µg/mL Pentamidine
25 µg/mL GO-Chi/Pent
50 µg/mL GO-Chi/Pent
100 µg/mL GO-Chi/Pent